

Temperature dependence of magnetic anisotropy in ferromagnetic (Ga,Mn)As films: Investigation by the planar Hall effect

D. Y. Shin, S. J. Chung, and Sanghoon Lee*
Physics Department, Korea University, Seoul 136-701, Korea

X. Liu and J. K. Furdyna
Physics Department, University of Notre Dame, Notre Dame, Indiana 46556, USA
 (Received 6 February 2007; revised manuscript received 25 April 2007; published 23 July 2007)

We carried out systematic planar Hall effect (PHE) measurements of GaMnAs ferromagnetic semiconductor film as a function of temperature. The two-step switching of the PHE occurring in the magnetization-reversal process was observed to change significantly as the temperature was increased. To investigate the mechanism responsible for such behavior, the temperature dependence of the PHE was continuously measured (with and without an external magnetic field) after the sample was first magnetized along one of the easy axes to produce an initial single-domain state at 3 K. A detailed temperature dependence of the magnetization direction was then obtained by taking the ratio of the planar Hall resistance measured with and without a magnetic field. As the temperature was increased, the direction of the easy axis of magnetization was observed to change from the [010] crystallographic direction to [110]. This reorientation of the easy axis direction can be understood in terms of the temperature dependence of the relative strengths of the magnetic anisotropy constants (i.e., of the ratio of uniaxial-to-cubic anisotropy) of the GaMnAs film.

DOI: [10.1103/PhysRevB.76.035327](https://doi.org/10.1103/PhysRevB.76.035327)

PACS number(s): 75.50.Pp, 75.70.-i, 75.60.-d, 75.47.-m

I. INTRODUCTION

The discovery of the magnetic properties of (Ga,Mn)As has opened up a new research field of carrier-mediated ferromagnetism,¹ and a great deal of experimental and theoretical work has already been devoted to the exploration of the fundamental properties of this and related III-Mn-V materials.² For example, the ability to electrically control ferromagnetism,³ enhanced planar Hall effect,⁴ and efficient spin injection into semiconductor nanostructures⁵ have already been demonstrated using ferromagnetic GaMnAs-based geometries. The enhancement of spin phenomena observed in this material provides a strong indication that spintronic device applications based on ferromagnetic semiconductors are indeed a strong possibility.

Among the many interesting properties of GaMnAs, phenomena arising from magnetic anisotropy are the most prominent—and probably the most important—from the viewpoint of practical spin memory device applications.^{6,7} A detailed investigation of the magnetic anisotropy in this material is therefore essential not only for the purpose of gaining a better understanding of the underlying physics, but also for practical reasons. It is known from earlier studies that the magnetic anisotropy (either in-plane or out-of-plane) of a GaMnAs film strongly depends on the strain within the film.^{8–10} Specifically, in a GaMnAs film under compressive strain the in-plane magnetic anisotropy is dominant; i.e., the system prefers to be magnetized within the plane. The actual orientation of the easy axis of magnetization within the plane will then depend on the relative values of the cubic and uniaxial anisotropy constants.⁴

Interestingly, the magnetic anisotropy constants of GaMnAs film are known to depend on temperature via changes in the carrier concentration.^{11,12} Magnetization measurements using a superconducting quantum interference device¹³

(SQUID) as well as magnetic imaging by high-resolution magneto-optical techniques¹⁴ have demonstrated a switching of the easy axes of magnetization between in-plane crystallographic directions (e.g., from [100] to [110] and vice versa) as the temperature was increased. The temperature dependence of the cubic and uniaxial anisotropy constants of GaMnAs was also obtained in those experiments. In the present paper we have undertaken a detailed study of the magnetic anisotropy of GaMnAs by electrical measurements, which are considerably simpler to carry out and thus provide a straightforward opportunity to obtain a very detailed mapping of the magnetic anisotropy parameters as a function of temperature.

Recently Tang *et al.*⁴ reported the observation of the giant planar Hall effect (PHE) in GaMnAs films and related the observed behavior directly to the magnetic anisotropy constants of the system. Even though the PHE measurement was shown to be very sensitive to the direction of magnetization, this feature was not fully utilized for investigating the temperature dependence of the magnetic anisotropy. In this study, we have adapted a technique of PHE measurement specifically for determining the temperature-dependent properties of the magnetic anisotropy in GaMnAs films. Specifically, by measuring the temperature-dependent planar Hall resistance (PHR) with and without an external magnetic field, we are able to obtain a detailed profile of the orientation of magnetization, from which the temperature-dependent changes of magnetic anisotropy parameters can be directly deduced.

II. SAMPLE FABRICATION AND EXPERIMENTAL PROCEDURE

The GaMnAs films studied in this investigation were prepared by molecular beam epitaxy (MBE) in a Riber 32 R&D

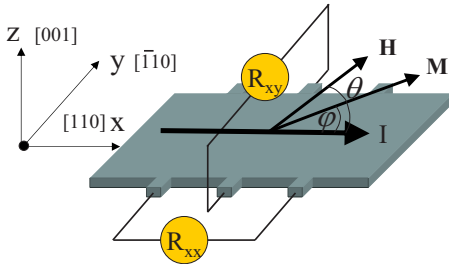


FIG. 1. (Color online) Schematic diagram of the Hall device geometry patterned on a GaMnAs film. The direction of current flow and the crystallographic directions are indicated on the diagram. The orientation of the magnetization (φ) and of the applied magnetic field (θ) are measured relative to the current direction.

MBE machine equipped with elemental sources Ga, Mn, and As. Prior to deposition of the GaMnAs film we grew a GaAs buffer layer at 600 °C on a (001) GaAs substrate. The substrate was then cooled to 220 °C for deposition of a 30-nm low-temperature (LT) GaAs buffer, followed by the growth of GaMnAs film. The Mn concentration of three GaMnAs films was 3.8%, 5.0%, and 6.4%, respectively. The entire growth process was monitored by reflection high-energy electron diffraction (RHEED), which showed a streaky (1×2) reconstruction pattern indicating smooth layer-by-layer growth. Since in this case the GaMnAs film is under compressive strain, the film possesses an in-plane magnetic anisotropy.^{8–10}

For transport measurements the GaMnAs films were patterned into Hall bars using photolithography and chemical wet etching. Although three GaMnAs films with different Mn concentrations were investigated, we mainly focus on results obtained on a single representative $\text{Ga}_{0.962}\text{Mn}_{0.038}\text{As}$ sample in this paper. However, we present the temperature dependence PHR data from all three samples in Fig. 3, below, to demonstrate the generality of observed results for GaMnAs samples. The representative Hall device is in the shape of a $400 \mu\text{m}$ by $2500 \mu\text{m}$ rectangle, with the long dimension along the $[110]$ direction and with six terminals for signal detection. A schematic diagram of the fabricated Hall device is shown in Fig. 1, where the crystallographic directions are indicated along with the voltage detection scheme. Magnetotransport measurements were performed using a He cryostat in which the temperature can be varied from 3 K to 300 K. The electromagnet was mounted on a stage designed such that a magnetic field could be applied in the plane of the sample at an arbitrary azimuthal angle. To eliminate noise in the detection of the Hall voltage we have used an ac current source and lock-in detection.

III. RESULTS AND DISCUSSION

A. Temperature-dependent planar Hall effect

The PHE data shown in Fig. 2(a) are obtained on a GaMnAs Hall device fabricated as described above. Each magnetic field scan is taken at a different temperature below the Curie temperature (T_c), with the magnetic field applied in the same azimuthal direction of $\theta=88^\circ$. In the hysteresis loops

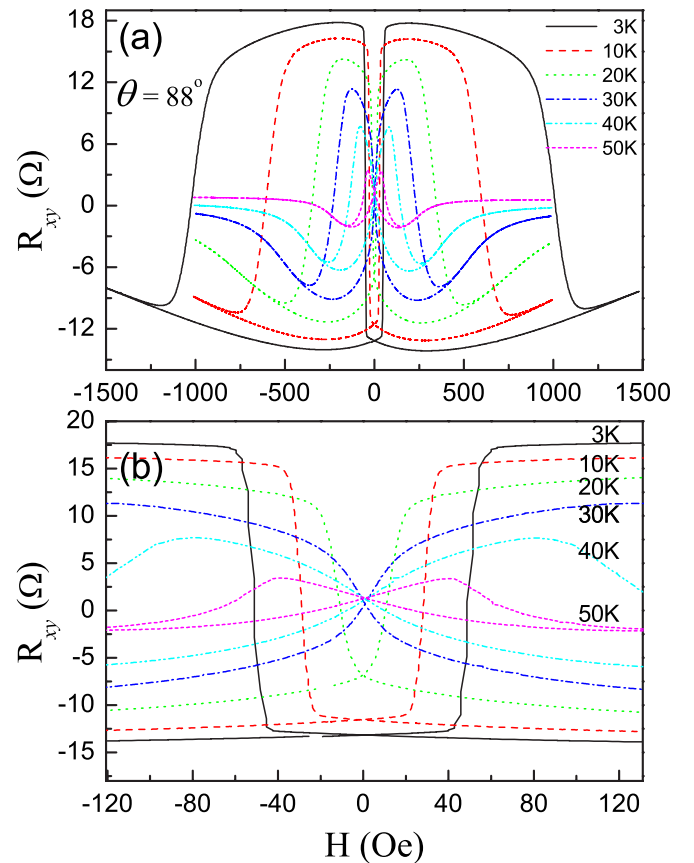


FIG. 2. (Color online) (a) Planar Hall resistance R_{xy} obtained in field scans at several different temperatures. A typical two-step switching behavior is clearly seen at low temperatures, but becomes significantly altered as the temperature increases. (b) A magnified view of the R_{xy} data in a narrow field range where the first magnetization switching occurs. Note that the R_{xy} values at zero magnetic field converge at $R_{xy}=0$ for all loops measured above 30 K.

taken at low temperatures four plateau regions are clearly defined, and a rather abrupt transition behavior is clearly observed in the magnetic field scans. The two-step switching phenomenon appearing in the hysteresis loops is well understood in terms of reorientation of magnetization in the magnetic system having four easy axes resulting from the dominance of the cubic anisotropy. Specifically, the easy axes of the specimen under investigation turn out to lie near the $[100]$, $[010]$, $[\bar{1}00]$, and $[0\bar{1}0]$ crystallographic directions, similar to the situation in our earlier study.¹⁵ Note that these easy axes are at about 45° relative to the direction of the current flow (the long dimension of the sample)—i.e., relative to the $[110]$ axis. The character of the PHE loops changes drastically as the temperature increases, indicating that thermal effects have a significant influence on the process of reorienting magnetization. Although such temperature-dependent behavior of the PHE has been observed in previous studies,⁴ no systematic analysis was attempted in interpreting the observed temperature effects, and in particular no correlation was made of these effects with the magnetic anisotropy properties of the system.

Here it must be emphasized that the value of the PHR R_{xy} is a very sensitive function to the direction of magnetization, as expected from the expression¹⁶

$$R_{xy}(M, J; \varphi) = \Delta R \cos \varphi \sin \varphi, \quad (1)$$

where M is the magnetization, J is the current density, φ is the angle between J and M , and ΔR is the difference between R_{\perp} and R_{\parallel} , R_{\perp} and R_{\parallel} being the resistances when the magnetization direction is perpendicular and parallel to the current flow, respectively. The observed PHR loops contain valuable information on the behavior of the magnetization direction, from which the magnetic anisotropy properties of the system can be understood. Measurements of the PHR can therefore automatically serve as a very effective experimental tool for studying in detail the properties of the magnetic anisotropy of the system.

To gain insight into the temperature-dependent properties of the magnetic anisotropy of the GaMnAs system from the PHE data, we focus on several interesting features of the data seen in Fig. 2. First, the transition between different magnetization orientations becomes less abrupt as the temperature increases [see the magnified view in Fig. 2(b)]. Second, the separation between the well-defined PHR states (i.e., the upper and lower plateaus) seen in the low-temperature data progressively collapses (i.e., the curves approach each other) as the temperature increases. And third, the values of the PHR at zero magnetic field systematically approach zero with increasing temperature and remain at zero in loops taken above 30 K. These temperature-dependent PHR feature data imply a strong relationship between PHE and magnetic anisotropy—an observation which is further supported by the additional temperature-dependent PHE experiments described below.

To correlate the PHR values and the direction of magnetization in a sample based on Eq. (1), the sample must be in the single-domain state, since a multidomain system can change the PHR value by superposing contributions from domains with different magnetization directions.¹⁵ In our experiments we used a 4000-Oe magnetic field, which is sufficiently strong to align the magnetization in the entire sample along the desired direction, thus producing a single-domain state. In the first experiment a field of 4000 Oe was applied at $\theta=45^\circ$ at 3 K so as to establish the direction of magnetization along [010] (i.e., near one of the easy axes of the sample), a geometry which yields the largest value of the PHR. The PHR (R_{xy}) and magnetoresistance (R_{xx}) were then measured simultaneously as the temperature was increased, and the magnetic field was kept at its original value of 4000 Oe. Since in this situation the direction of magnetization remains “pinned” along the direction of the (strong) external field during the measurements, the observed values of R_{xy} and R_{xx} do not change significantly as the temperature is increased. The data for R_{xy} and R_{xx} obtained in this condition are shown as dotted lines in Fig. 3 (R_{xy} left axis; R_{xx} right axis) for three GaMnAs samples. Since the temperature behaviors of R_{xy} and R_{xx} observed in the three samples are very similar, we will only discuss data shown in Fig. 3(a) in the following. The position of the hump appearing in the R_{xx} spectrum indicates that the T_c of the sample is approximately

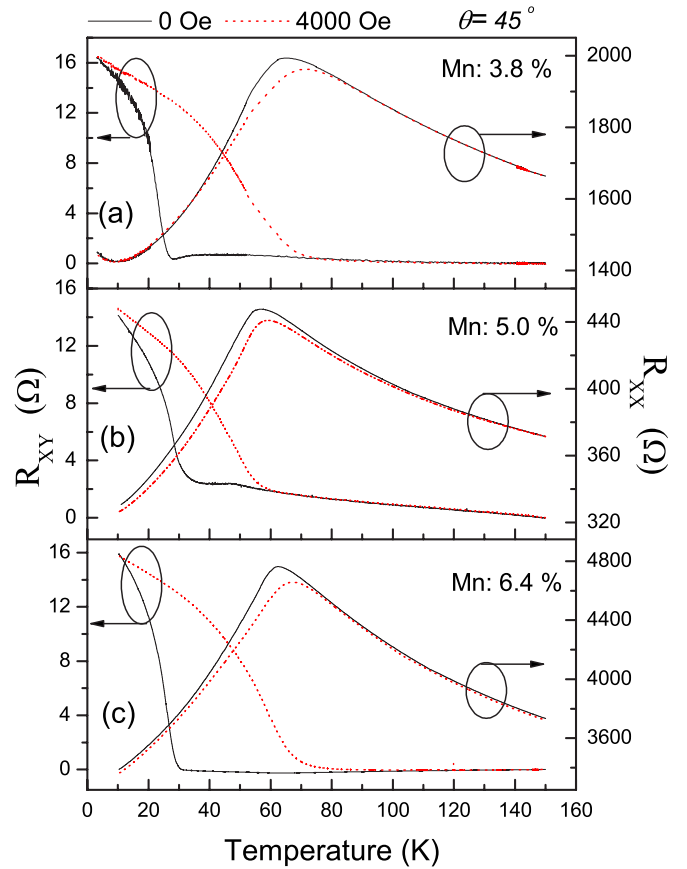


FIG. 3. (Color online) Continuous changes of R_{xy} and R_{xx} as a function of temperature. Panels (a), (b), and (c) represent, respectively, GaMnAs samples with Mn concentration of 3.8%, 5.0%, and 6.4%. The dotted and solid lines represent data taken with and without a magnetic field after magnetization is “primed” by applying a 4000-Oe field along an easy axis (i.e., along the [010] direction). The drop of R_{xy} to zero at a much lower temperature than T_c is clearly seen in the data taken with no field.

70 K.^{17,18} The value of R_{xy} taken in the presence of a magnetic field shows a monotonic decrease with increasing temperature, reaching zero at the temperature where a peak is seen in the R_{xx} data. The respective temperature behaviors of R_{xy} and R_{xx} obtained in the presence of a strong magnetic field are consistent with the decrease of magnetization of the sample observed as the temperature increases.

In the second experiment we have magnetically “primed” the sample by using the same procedure as in the first experiment (i.e., applying 4000 Oe at $\theta=45^\circ$). The field was then removed, and the values of R_{xy} and R_{xx} were measured simultaneously in the absence of a field as the temperature was increased. The R_{xy} and R_{xx} values obtained in this experiment are shown as solid lines in Fig. 3(a). The value of T_c for the sample appears to be slightly lower (i.e., near 62 K) compared to that seen in the data taken in a magnetic field of 4000 Oe. This small difference in T_c measured with and without a magnetic field can be ascribed to the difference in the degree of magnetic alignment within the system in the two situations.¹⁹ The difference in the behavior of the data taken with and without an external field is especially evident in R_{xy} (see left axis of Fig. 3). It is very interesting that the

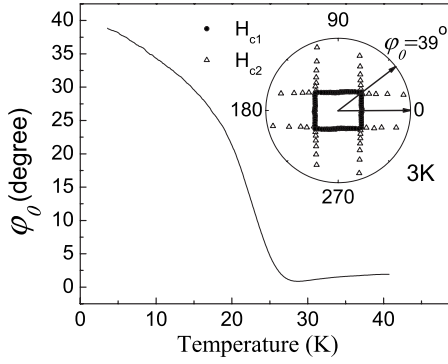


FIG. 4. Direction of the easy axis of magnetization φ_0 as a function of temperature. At 3 K the easy axis direction is at 39° (i.e., near the [010] direction), the same angle as that determined from the angle-dependent switching field data shown in the inset. It is clear from the data that the easy axis direction monotonically approaches $\varphi_0=0$ (i.e., the [110] direction), reaching $\varphi_0=0$ at 26 K (i.e., at a much lower temperature than T_c which is around 62 K for this sample).

value of R_{xy} measured without a magnetic field drops much more rapidly compared to that obtained with the field on and goes to zero at 26 K—i.e., well below the T_c appearing in the corresponding R_{xx} data. This behavior is consistent with the third feature pointed out above in connection with Fig. 2 (i.e., that the value of R_{xy} measured in the field sweeps shown in Fig. 2 converges to zero for 26 K at zero field). Since the magnetization of the GaMnAs film is not zero at temperatures below T_c of the system (i.e., below 62 K), the fact that the measured value of R_{xy} drops to zero at a temperature well below T_c must be related to a change of the magnetization direction [see Eq. (1)] as the temperature is increased.

Valuable information regarding the direction of magnetization at zero field can be obtained from the ratio of PHR values measured with and without a magnetic field. Using Eq. (1), the ratio can be expressed as²⁰

$$\frac{R_{xy}(H) - R_{xy}(H=0)}{R_{xy}(H=0)} = \frac{\sin 2\varphi_H - \sin 2\varphi_0}{\sin 2\varphi_0}, \quad (2)$$

where φ_H and φ_0 represent the angle between J and M in the presence and absence of H , respectively, and $R_{xy}(H)$ and $R_{xy}(H=0)$ are the respective values of R_{xy} measured with and without a magnetic field. Since the direction of magnetization at zero field corresponds to the angle φ_0 , one can directly obtain the orientation of magnetization as a function of temperature if the angle φ_H is fixed. As described above, data $R_{xy}(H)$ were obtained under an external magnetic field of 4000 Oe, which is sufficiently strong to “pin” the direction of magnetization along the field direction (i.e., $\varphi_H = \theta = 45^\circ$). This then allows us to experimentally determine the temperature-dependent direction of magnetization of the sample using Eq. (2) and the data in Fig. 3.

Figure 4 shows the temperature-dependent direction of magnetization as given by the angle φ_0 . Since the magnetization at zero field can be assumed to lie along the easy axis, the temperature profile of the angle φ_0 shown in Fig. 4 au-

tomatically provides the temperature behavior of the easy axis of the system. The value of the angle φ_0 at 3 K appears to be about 39°, which is slightly deviated from the [010] direction. Although we first aligned the direction of magnetization along [010] with a strong magnetic field, it will relax to the exact easy axis direction of the sample when the field is removed. Such a deviation of the easy axis indicates an interplay between the cubic and uniaxial anisotropy already at 3 K, which will be discussed in more detail in the following section.

This value $\varphi_0=39^\circ$ at 3 K is indeed consistent with the direction of the easy axis determined from the angular dependence of the magnetization switching fields referred to as H_{c1} and H_{c2} ²¹ (Ref. 21) in the inset of Fig. 4. The agreement of the easy axis direction at 3 K obtained by two different methods provides strong support for the reliability of our analysis based on Eq. (2). The angle φ_0 monotonically changes from the initially set direction near [010] (i.e., $\varphi_0 = 39^\circ$) at 3 K toward the [110] direction (i.e., $\varphi_0=0$) with increasing temperature. This clearly indicates that the direction of the magnetic easy axis continuously rotates from near [010] to [110] with increasing temperature up to 26 K and above that temperature it remains fixed at the [110] direction until the ferromagnetism of the sample disappears at T_c . This change of magnetic easy axis can be understood based on the temperature-dependent magnetic anisotropy of the system, as discussed in the following section.

B. Temperature-dependent anisotropy constants

The relationship between magnetic anisotropy and the orientation of magnetization can be described by the magnetic free energy. Using the Stoner-Wohlfarth model, the free energy of an in-plane magnetized sample is given by⁴

$$E = K_u \sin^2 \varphi + (K_c/4) \cos^2 2\varphi - MH \cos(\varphi - \theta), \quad (3)$$

where K_u and K_c are the uniaxial and cubic anisotropy constants, respectively, and φ and θ are the angles of magnetization and of the external magnetic field directions measured from [110]. Since [110] is the direction of the current flow (see Fig. 1), the angle φ in Eq. (3) is the same angle as that in Eq. (1) which describes the angular dependence of R_{xy} . The positions of the energy minima determined from Eq. (3) give the directions of magnetization for any given situation. At zero magnetic field [in this case φ becomes φ_0 , as in Eq. (2)], the relative values of the two anisotropy constants in Eq. (3) play a key role in determining the positions of the energy minima. In Fig. 5 we plot the free energy in the absence of a magnetic field [i.e., $H=0$ in Eq. (3)] as a function of the angle φ_0 for different ratios of the cubic (K_c) and uniaxial (K_u) anisotropy constants, as indicated on the left side of each panel in the figure.

In the complete absence of a uniaxial anisotropy contribution, the energy minima appear at $\varphi_0 = -45^\circ$ and $\varphi_0 = 45^\circ$, corresponding to the [100] and [010] crystallographic directions, as seen in the top panel. The positions of the energy minima monotonically shift toward $\varphi_0 = 0^\circ$ (i.e., toward the [110] direction) as the uniaxial contribution increases. When the contributions from the uniaxial and cubic anisotropy con-

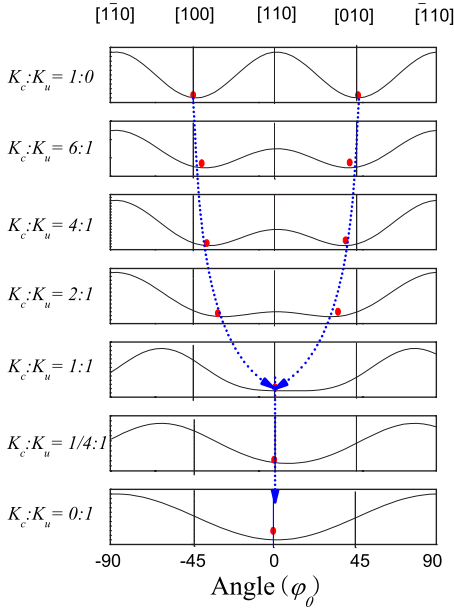


FIG. 5. (Color online) Magnetic free energy given by Eq. (3), plotted as a function of φ_0 . When $K_u:K_c=1:0$, the energy minimum positions appear at $\varphi_0=\pm 45^\circ$ —i.e., at [010] and [100] directions, respectively, as shown in the top panel. The free energy minima gradually shift toward the [110] direction as the weight of K_u increases in Eq. (3), reaching the [110] direction when $K_u:K_c=1:1$. The minimum position then remains the same angle irrespective of further increase of the relative weight of K_u . The behavior of the energy minima with changing K_u/K_c ratio is the underlying mechanism of the behavior of magnetization direction with changing temperature seen in Fig. 4.

stants become equal, the positions of the two energy minima are seen to merge at $\varphi_0=0^\circ$. Any further increase of the uniaxial contribution only lowers the value of the energy, but does not change the position of the energy minimum. Such anisotropy-dependent behavior of energy minima is similar to the temperature behavior of the magnetization angle φ_0 seen in Fig. 4. Thus the observed change of the preferred direction of magnetization with increasing temperature can be understood in terms of changes in the anisotropy constants produced by the changing temperature.

The exact positions of the energy minima can be found by differentiating Eq. (3) with respect to angle φ , as shown below:

$$\frac{\partial E}{\partial \varphi} = MH \sin(\varphi - \theta) + \frac{1}{2}M(H_u - H_c \cos 2\varphi)\sin 2\varphi = 0, \quad (4)$$

in which we introduce the uniaxial and cubic anisotropy fields, defined as $H_u=2K_u/M$ and $H_c=2K_c/M$. Equation (4) leads to the relation $\varphi=\frac{1}{2}\cos^{-1}(K_u/K_c)$ for the directions of energy minima at zero magnetic field.²¹ Using this relation together with data shown in Fig. 4, one can then obtain the temperature-dependent anisotropy ratio K_u/K_c . The values of K_u/K_c obtained in this way are plotted as a solid line in Fig. 6, where the ratio is seen to increase monotonically with increasing temperature. The values of K_u/K_c are plotted only

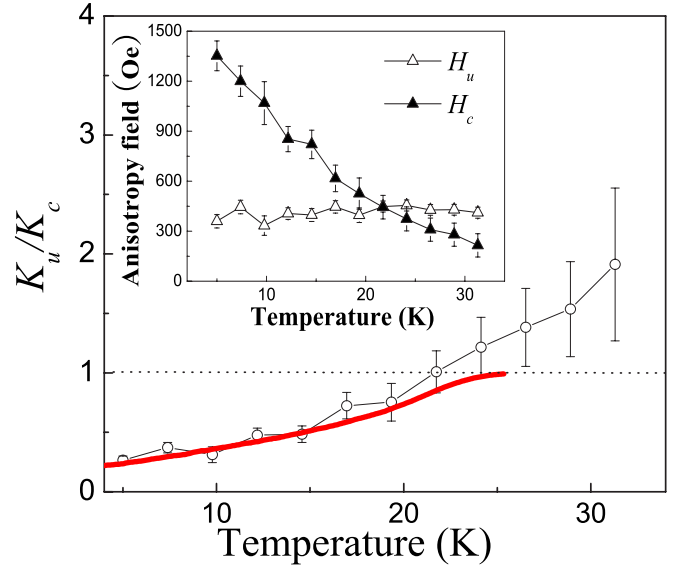


FIG. 6. (Color online) Temperature-dependent values of K_u/K_c obtained from PHE measurements. The thick solid line represents the values obtained directly from experimental results shown in Fig. 4. The values plotted as open circles are obtained by fitting the observed angular dependence of the PHR, which independently yields the values of K_u/M and K_c/M (shown in the inset). It is noteworthy that the results from the temperature dependence and angular dependence of PHR experiments show the same temperature behavior and quantitatively agree within experimental error.

to 26 K, since the relation $\varphi=\frac{1}{2}\cos^{-1}(K_u/K_c)$ can lead to incorrect information due to $\varphi=0^\circ$ above 26 K, by implying that the ratio $K_u/K_c=1$ above that temperature, whereas the anisotropy constants do actually change in that temperature range, as has been observed in other measurements.^{13,14} This is because Eq. (4) determines energy minimum position and the increase of the K_u/K_c value over 1 only lowers the value of the energy in Eq. (3) without changing the position of the energy minimum.

We have further checked the temperature-dependent behavior of the magnetic anisotropy by measuring the angular dependence of R_{xy} , from which the cubic and uniaxial anisotropy fields (i.e., H_u and H_c) can be independently obtained for different temperatures by using the fitting process described in Ref. 22. This experiment reveals that H_c is more than 4 times larger than H_u at 3 K, as shown in the inset of Fig. 6. While the value of H_c decreases very rapidly with increasing temperature, H_u is rather insensitive to the temperature. Owing to such different temperature dependences of the two anisotropy constants, their relative strengths reverse around 26 K in our experimental conditions. The values of K_u/K_c were calculated from the data shown in the inset in Fig. 6 and are plotted as open circles in the figure. The temperature behavior of the anisotropy constant ratio obtained from the experimental angular dependence of PHR is consistent with that obtained from direct observation of magnetic domain orientation through the temperature-dependent PHR measurements. This experiment therefore confirms the strong temperature dependence of the anisotropy constants in a GaMnAs film, as well as the capability

of PHR measurements to continuously monitor the orientation of the magnetization.

IV. CONCLUSION

In this study we have used transport measurements for the purpose of investigating the behavior of magnetic anisotropy constants in thin GaMnAs layers as a function of temperature. Specifically, this technique enabled us to continuously monitor the orientation of magnetization by measuring the planar Hall effect, which provides direct information on the direction of the magnetic easy axis in a ferromagnetic film. The easy axis was found to lie near the [010] direction of the GaMnAs crystal film at 3 K and gradually reoriented toward the [110] direction as the temperature increased. This behavior could be understood in terms of the variations in cubic and uniaxial anisotropy constants with increasing temperature. The ratio of the uniaxial-to-cubic anisotropy constants (i.e., K_u/K_c) was obtained directly from experimental data, without any fitting process. The value of K_u/K_c monotonically

increases with increasing temperature, as has also been observed in earlier studies based on other experimental techniques.^{13,14,23,24} We have also compared the temperature dependence of K_u/K_c obtained in this way with the results obtained independently by measuring the angular dependence of the planar Hall effect at a high magnetic field. The K_u/K_c values obtained by these two different methods not only have the same temperature trends, but show quantitative agreement within experimental error. Thus the results of this paper demonstrate that transport measurements, and in particular the PHE, can serve as a powerful tool for studying the magnetic anisotropy in thin ferromagnetic semiconductor films.

ACKNOWLEDGMENTS

This work was supported by Korea Research Foundation Grant No. KRF-2004-005-C00068, by the Seoul R&DB Program, by the KOSEF through QSRC at Dongguk University, and by the National Science Foundation through Grant No. DMR06-03762.

*Electronic address: slee3@korea.ac.kr

¹H. Ohno, *Science* **281**, 951 (1998).

²T. Dietl *et al.*, *Science* **287**, 1019 (2000).

³H. Ohno *et al.*, *Nature (London)* **408**, 944 (2000).

⁴H. X. Tang, R. K. Kawakami, D. D. Awschalom, and M. L. Roukes, *Phys. Rev. Lett.* **90**, 107201 (2003).

⁵Y. Ohno *et al.*, *Physica E (Amsterdam)* **10**, 489 (2001).

⁶W. L. Lim, X. Liu, K. Dziatkowski, Z. Ge, S. Shen, J. K. Furdyna, and M. Dobrowolska, *Phys. Rev. B* **74**, 045303 (2006).

⁷Y. Bason *et al.*, *Appl. Phys. Lett.* **84**, 2593 (2004).

⁸T. Dietl, *Physica E (Amsterdam)* **10**, 120 (2001).

⁹M. Sawicki *et al.*, *J. Supercond.* **16**, 7 (2003).

¹⁰X. Liu, Y. Sasaki, and J. K. Furdyna, *Phys. Rev. B* **67**, 205204 (2003).

¹¹M. Sawicki, F. Matsukura, A. Idziaszek, T. Dietl, G. M. Schott, C. Rueter, C. Gould, G. Karczewski, G. Schmidt, and L. W. Molenkamp, *Phys. Rev. B* **70**, 245325 (2004).

¹²T. Dietl, H. Ohno, and F. Matsukura, *Phys. Rev. B* **63**, 195205 (2001).

¹³K.-Y. Wang, M. Sawicki, K. W. Edmonds, R. P. Campion, S. Maat, C. T. Foxon, B. L. Gallagher, and T. Dietl, *Phys. Rev.*

Lett. **95**, 217204 (2005).

¹⁴U. Welp, V. K. Vlasko-Vlasov, X. Liu, J. K. Furdyna, and T. Wojtowicz, *Phys. Rev. Lett.* **90**, 167206 (2003).

¹⁵D. Y. Shin, S. J. Chung, Sanghoon Lee, X. Liu, and J. K. Furdyna, *Phys. Rev. Lett.* **98**, 047201 (2007).

¹⁶T. R. Mcguire and R. I. Potter, *IEEE Trans. Magn.* **11**, 1018 (1975).

¹⁷Sh. U. Yuldasheva, Hyunsik Imb, V. Sh. Yalisheva, C. S. Park, T. W. Kang, Sanghoon Lee, Y. Sasaki, X. Liu, and J. K. Furdyna, *Appl. Phys. Lett.* **82**, 1206 (2003).

¹⁸E. L. Nagaev, *Phys. Rep.* **346**, 387 (2001).

¹⁹H. Ohno *et al.*, *Physica E (Amsterdam)* **2**, 904 (1998).

²⁰C.-R. Chang, *IEEE Trans. Magn.* **36**, 1214 (2000).

²¹Yong Pu, E. Johnston-Halperin, D. D. Awschalom, and Jing Shi, *Phys. Rev. Lett.* **97**, 036601 (2006).

²²T. Yamada, D. Chiba, F. Matsukura, S. Yakata, and H. Ohno, *Phys. Status Solidi C* **3**, 4086 (2006).

²³L. V. Titova, M. Kutrowski, X. Liu, R. Chakarvorty, W. L. Lim, T. Wojtowicz, J. K. Furdyna, and M. Dobrowolska, *Phys. Rev. B* **72**, 165205 (2005).

²⁴V. Stanciu and P. Svedlindh, *Appl. Phys. Lett.* **87**, 242509 (2005).